NJC

New Journal of Chemistry

An international journal of the chemical sciences

www.rsc.org/njc

Volume 33 | Number 10 | October 2009 | Pages 1981–2184

ISSN 1144-0546

RSC Publishing

PAPER

Pauline M. Schwartz *et al.*

Systems chemistry and Parrondo's paradox: computational models of thermal cycling

Systems chemistry and Parrondo's paradox: computational models of thermal cycling

Daniel C. Osipovitch,[a] Carl Barratt[b] and Pauline M. Schwartz*[a]

Received (in Gainesville, FL, USA) 7th January 2009, Accepted 1st May 2009
First published as an Advance Article on the web 1st June 2009
DOI: 10.1039/b900288j

A mathematical concept known as Parrondo's paradox motivated the development of several novel computational models of chemical systems, in which thermal cycling was explored. In these kinetics systems, we compared the rates of formation of products under temperature-cycling and steady-state conditions. We found model chemical systems that counter-intuitively predicted a greater concentration of product under oscillating temperature conditions than under fixed conditions. At a practical level, these computational models of thermal cycling suggest new applications in chemistry, biochemistry and chemical engineering. More fundamentally, these models contribute to a growing understanding that even simple chemical systems may behave paradoxically, and that forced oscillating conditions may induce such an outcome.

Introduction

Systems chemistry is an important niche discipline that investigates the behavior of interacting chemical reactions.[1,2] Like systems biology and systems engineering, a critical feature of systems chemistry is that unexpected outcomes may arise that may not have been predicted by examining the behavior of the individual components of the system. Complex behaviors can arise over time from even simple systems. Recent efforts have focused on breaking symmetry in chemical systems to understand the generation of homochirality in prebiotic environments. Systems chemistry will undoubtedly play a role in the future of organic chemistry.[3]

The counter-intuitive mathematical concept known as Parrondo's paradox is an intriguing starting point to inspire the development of chemical model systems. Parrondo's paradox is the unexpected situation in which two specific losing strategies can, by alternating between them, produce a winning outcome.[4–6] The complex statistical elements of Parrondo's paradox are often demonstrated by means of gambling games. Fig. 1 shows the outcome of the most simple form of Parrondo's paradox using modulo 2 (MOD 2); in this case, the outcomes of the two strategies (games A or B played alone) are "losing" but if the games are played alternately (A, B, A, B...), paradoxically the result is a "winning" outcome. Briefly, the simple game, game A, is defined with a greater probability for the losing outcome. Game B is a more complex game with two arms; game B played alone is an overall losing situation, although one of its arms is a winning outcome. The paradox arises by "filtering out" the losing arm of game B and accentuating the winning arm. Parrondo's paradox can be demonstrated over a wide range of probabilities and selections of modulo operations that define game B. In the case shown in Fig. 1, the MOD 2 condition is used with the alternating games (A, B, A, B...). A more complete description of the mathematics behind Parrondo's paradox and links to informative animations can be found at The University of Adelaide, School of Electrical Engineering, Official Parrondo's Paradox web page.[7]

Parrondo's paradox has generated a significant amount of activity since its first presentation in 1999.[4–11] One of the earliest extensions was to use Parrondo's strategy to develop a relationship with the paradoxical behavior of Brownian ratchets. The inherent mechanism is described in some physical systems as the "rectification of noise" contributing to an unexpected outcome. An interesting variation of a Parrondo's paradox-based game was described by Martin and von Baeyer, who posited that two slowly winning games could be combined to generate a fast winning game.[11] Systems that demonstrate such paradoxical outcomes are understood in terms of the interactions of simple components, where non-linear, asymmetric behavior emerges. Importantly,

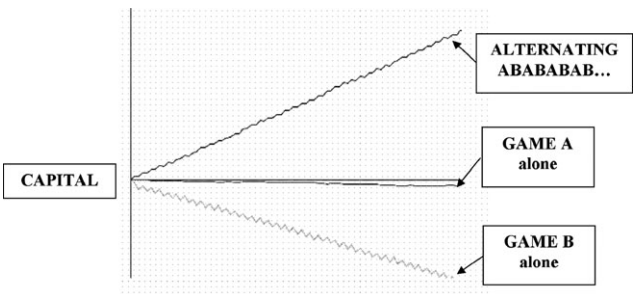

Fig. 1 An example of results from a typical set of 500 games demonstrating Parrondo's paradox. The outcomes were generated by from a web applet (http://www.cut-the-knot.org/ctk/Parrondo.shtml). Games A, B and alternating strategy ABABAB... were played using the following parameters: modulus 2, $\varepsilon = 0.005$, $P = 0.5$, $P1 = 0.1$ and $P2 = 0.75$. Parameters and probabilities are defined in ref. 5.

[a] *Department of Chemistry and Chemical Engineering, Tagliatela College of Engineering, University of New Haven, West Haven, CT 06516, USA. E-mail: pschwartz@newhaven.edu; Fax: +1 203-931-6077; Tel: +1 203-932-7170*
[b] *Department of Mechanical, Civil and Environmental Engineering, Tagliatela College of Engineering, University of New Haven, West Haven, CT 06516, USA*

applications of Parrondo's paradox do not violate the second law of thermodynamics, despite the "something-for-nothing" impression.

Our studies focused on finding a chemical analog to Parrondo's paradox—discovering a system of hypothetical chemical reactions that would produce a higher yield of a product when switching between conditions, compared to steady-state conditions.

Results and discussion

A simple stochastic chemical model based on Parrondo's paradox

To mimic the game strategies of Parrondo's paradox, a reaction scheme was devised with the production of alternate products from a common reactant, **A**. Product **B** is considered the "losing" product and product **C** is considered the "winning" product. The reaction could be conducted under condition I, condition II or an alternating pattern of conditions, *i.e.* I, II, I, II, I, II... Table 1 describes some basic relationships between the game strategy that underlies Parrondo's paradox and this simple stochastic model chemical system.

A typical reaction strategy that is analogous to a Parrondo's scheme is shown in Fig. 2, in which **B** is the "losing" product and **C** is the "winning" product. The objective was to devise a chemical model analogous to the paradoxical case, in which two slowly winning games (slow overall rate of accumulation of target product **C**) can be combined to give a fast winning game (fast overall rate of accumulation of target product **C**).[11] In this case, condition I is the alternate conversion of reactant **A** to products **B** or **C** following "probabilities" for each step, analogous to relative reaction rates. In condition I, the relative rate for the formation of **B** is greater than that for the formation of **C**; thus, for condition I, the production of **B** is favored over the production of product **C**. Condition II has two arms, in each of which reactant **A** is converted to products **B** or **C**. In condition II, the relative rates depend on the presence of a catalyst (the formation of **C** is faster than **B**) or inhibitor (the formation of **B** is faster than **C**). For condition II alone, the overall rate of formation of **B** is greater than the rate of formation of **C**; *i.e.*, "played" alone, **B** is the probable product. If the relative reaction rates are chosen properly (as they are in this example), then under oscillating conditions, the formation of **C** under the catalytic arm of condition II is continually selected, and the rate of formation of **C** is enhanced by changing between condition I and the catalytic arm of condition II.

A simple Excel program was created using the program's random number generator to calculate the accumulation of alternate products **B** and **C** from starting compound **A**, and mimicking the game strategies of Parrondo's paradox. The program calculated the accumulation of products after 1000 iterations, *i.e.* reactive interactions converting molecule **A** to products **B** or **C**. The model is stochastic because the relative rates are calculated at each iteration based on the probabilities determined by the random number generator. Fig. 3 shows the accumulation of **B** and **C** with condition I alone, condition II alone and oscillating conditions. In this model, more molecule **C** accumulates under the oscillating conditions than under either steady state.

Deterministic chemical models of Parrondo's paradox

In the initial model, conditions I and II could be various types of conditions. For the deterministic models, oscillating the temperature was used to mimic alternating conditions because reaction kinetic equations are easy to model. We designed two models, in which we could explore the possibility of paradoxical behavior of a chemical system operating under thermal cycling, as opposed to fixed temperature conditions. The **ABC** model was developed as a simple chemical system that is a multi-step pathway catalyzed by a temperature-sensitive catalyst (Fig. 4). The system is a feedback, auto-catalytic set of reactions, in which the catalyst is active at a low temperature (**Y**) and inactive at high temperature (**X**). The chemical model is described in Fig. 4. The reactants in the **ABC** model are **A** and **B**, with **A** as an isomer of **B**; **C** is the target product.

These reactions and their kinetic constants were input into the Kintecus 3.953 program. Kintecus is a powerful simulation program for chemical dynamics developed by J. C. Ianni and is free for academic use.[12] As a deterministic, Arrhenius-based program, the inputs include: the reaction steps, energies of activation, Arrhenius constants, reactant concentrations and temperature profiles. The program assumes elementary reaction steps and solves numerically for the differential equations of the related rate laws. The concentrations of participating species are calculated and displayed over time at either a fixed temperature or under varying temperature conditions. We describe here a typical set of conditions for the **ABC** model which highlight the paradoxical behavior that occurs under cycling temperature conditions (Fig. 4). The initial concentrations are [**A**] = 1 M (constant), [**B**] = 1×10^{-4} M and [**X**] = 1×10^{-3} M.

Fig. 5 shows the time course of the formation of **C** at fixed temperatures of 300 and 480 K, and with thermal cycling; also

Table 1 Relationships between Parrondo's paradox strategies and a model chemical system

Parrondo's paradox game strategy	Stochastic model of chemical system
Games A/B	Conditions I/II
Winning outcome	Accumulation of product **C**
Losing outcome	Accumulation of product **B**
Probabilities	Relative reaction rates
ABABAB... switching	Conditions I/II: oscillating conditions (temperature, light/dark, pH, *etc.*)
Games B1 *vs.* B2	Condition II: catalyzed *vs.* inhibited pathways
MOD2	Activity of "catalyst" *vs.* "inhibitor"

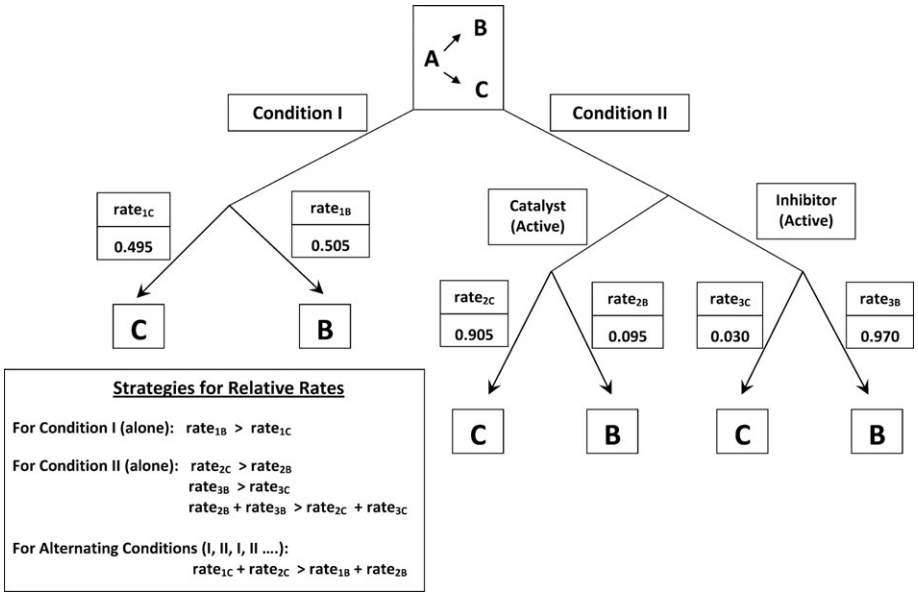

Fig. 2 Typical probabilities (relative rates) for the conversion of **A** to **B** or **C** in a stochastic model of a chemical system displaying behavior analogous to Parrondo's paradox.

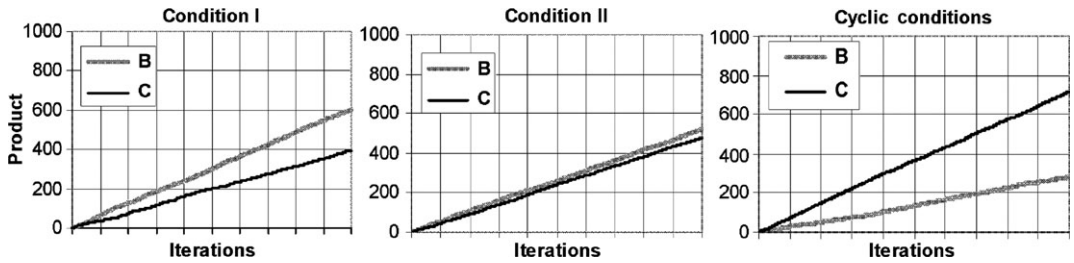

Fig. 3 The accumulation of products **B** and **C**, as predicted from the stochastic model (Fig. 2.) under condition I alone, condition II alone or oscillating between conditions I and II.

Reaction Step	A	E_a	k (at 300K)	k (at 480K)
(1) A + B ⟶ C	20.0	50.0	3.94×10^{-8}	7.25×10^{-5}
(2) A + B + Y ⟶ C + Y	20.0	1.0	1.34×10^{1}	1.56×10^{1}
(3) C ⟶ 2 B	1.0	18.0	7.34×10^{-4}	1.10×10^{-2}
(4) X ⟶ Y	1.0	7.0	6.04×10^{-2}	1.73×10^{-1}
(5) Y ⟶ X	100.0	12.0	8.14×10^{-1}	4.94×10^{0}

Initial Concentrations
[X] = 1.0×10^{-3} M
[Y] = 0.0 M
[A] = 1.0 M (constant)
[B] = 1.0×10^{-4} M
[C] = 0.0 M

Fig. 4 A description of the **ABC** model. Inputs include reaction steps, kinetic parameters, A (the Arrhenius constant), E_a and initial concentrations.

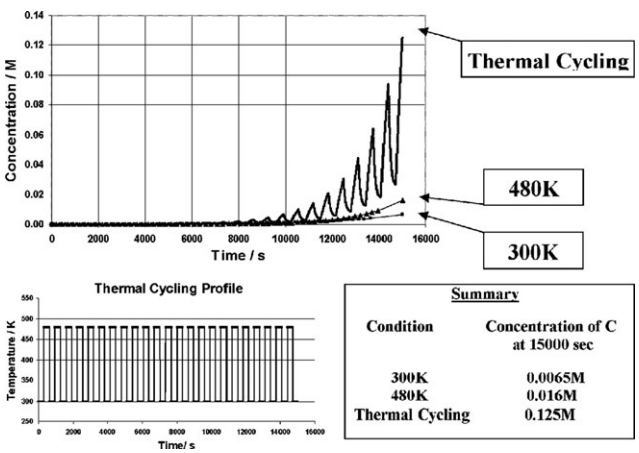

Fig. 5 Predictions from the **ABC** model. The results include the concentrations of target product **C** after the model has been run under fixed temperature conditions (300 and 480 K) or under a thermal cycling profile. The cycle time is 640 s, with equal time spent at 300 and 480 K. There are 23 cycles, and temperatures begin and end at 300 K over the 15 000 s time course.

shown is the cycling temperature profile for this model. The cycling temperature conditions drive oscillations of the concentrations of **X** and **Y**, which in turn generates an asymmetrical oscillating increase in the concentration of **C**. The model predicts that at 300 K, 6.5×10^{-3} M **C** would be generated in 15 000 s, and at 480 K, 1.6×10^{-2} M **C** would be generated in the same time frame. However, under oscillating temperatures (23 cycles in 15 000 s), considerably more **C** is formed, and 1.25×10^{-1} M **C** is generated. More **C** is produced under oscillating temperature conditions than under any steady state temperature between 300 K and 480 K (Fig. 6). In the example described in Fig. 5, the concentration

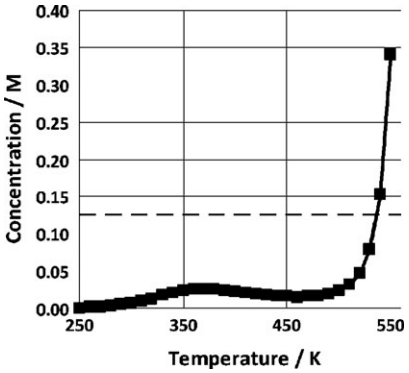

Fig. 6 The concentration of product **C** predicted from the **ABC** model (Fig. 4 and Fig. 5) at fixed temperatures from 250 to 550 K compared to thermal cycling (dashed line).

of **C** results from a square wave temperature profile, which is easiest to analyze numerically (see the next section). Similar results were obtained with a sinusoidal oscillating temperature profile.

The paradoxical outcome of this model system was verified by an examination of the differential equations that describe the rate laws for the different steps of the reaction under different temperature profiles. The reactions

$$X \xrightarrow{k_1} Y$$

$$Y \xrightarrow{k_2} X$$

$$C \xrightarrow{k_3} 2B$$

$$A + B + Y \xrightarrow{k_4} C + Y$$

$$A + B \xrightarrow{k_5} C$$

may be modelled using the following kinematic reaction equations:

$$\mathrm{d}X/\mathrm{d}t = -k_1X + k_2Y$$

$$\mathrm{d}Y/\mathrm{d}t = -k_2Y + k_1X$$

$$\mathrm{d}B/\mathrm{d}t = 2k_3C - k_4ABY - k_5AB$$

$$\mathrm{d}C/\mathrm{d}t = -k_3C + k_4ABY + k_5AB$$

$$\mathrm{d}A/\mathrm{d}t = -k_4ABY - k_5AB$$

where the concentration of A is constant, as in this model, ($\mathrm{d}A/\mathrm{d}t = 0$), X represents the molar concentration of chemical **X** (initial value X_0), *etc*., and the reaction constants k_1 to k_5 are obtained in the usual way using the Arrhenius equation:

$$k = AT^m\, \mathrm{e}^{(-E_a/RT)}$$

where A is the Arrhenius constant, E_a is the energy of activation, R is the gas constant (0.008315 kJ mol^{-1} K^{-1}) and T is the absolute temperature; in the model systems, the temperature coefficient, m, is zero. The reader should distinguish between A the Arrhenius constant, and **A** the reactant and its concentration. The X,Y equations are easily solved to yield:

$$Y(t) = [X_0(1 - \mathrm{e}^{-(k_1+k_2)t}) + Y_0(1 + (k_2/k_1)\mathrm{e}^{-(k_1+k_2)t})]/(1 + k_2/k_1)$$

$$X(t) = [X_0(k_2/k_1 + \mathrm{e}^{-(k_1+k_2)t}) + (k_2/k_1)Y_0(1 - \mathrm{e}^{-(k_1+k_2)t})]/(1 + k_2/k_1)$$

In chemical applications in which temperature is kept constant, k_1 and k_2 are usually such that X and Y very quickly "flatline," *i.e*., within seconds they acquire a constant value as equilibrium is reached. Under this assumption, together with the assumption that the concentration of chemical **A** is constant, the differential equations may also be solved to yield:

$$(\alpha_1 - \alpha_2)B(t) = B_0(\alpha_1\mathrm{e}^{-k\prime_4(1-\alpha_2)t} - \alpha_2\mathrm{e}^{-k\prime_4(1-\alpha_1)t}) + \alpha_1\alpha_2C_0(\mathrm{e}^{-k\prime_4(1-\alpha_2)t} - \mathrm{e}^{-k\prime_4(1-\alpha_1)t})$$

$$(\alpha_1 - \alpha_2)C(t) = B_0(\mathrm{e}^{-k\prime_4(1-\alpha_1)t} - \mathrm{e}^{-k\prime_4(1-\alpha_2)t}) + C_0(\alpha_1\mathrm{e}^{-k\prime_4(1-\alpha_1)t} - \alpha_2\mathrm{e}^{-k\prime_4(1-\alpha_2)t})$$

in which the constants α_1 and α_2 are obtained using:

$$k'_4 = k_4A[(X_0 + Y_0)/(1 + k_2/k_1)] + k_5A$$

$$\eta = k_3/k'_4$$

$$2\alpha_{1/2} = 1 - \eta \pm \sqrt{(1-\eta)^2 + 8\eta}$$

The above limiting solutions of the reaction equations are found to fit the Kintecus numerical solution exactly. As calculated by the Kintecus program, the solutions correspondingly predict a significant increase in the production of **C** when the temperatures oscillate according to T_1, T_2, T_1, T_2...

As noted, the temperature profile for the **ABC** model cycles between 300 and 480 K (Fig. 5). No steady state temperature between 300 and 480 K predicts more product **C** than thermal cycling, and an excessively high temperature of 540 K would be needed to generate as much product over the given time course as thermal cycling (Fig. 6). In addition, increasing the frequency of thermal cycling has a significant effect on

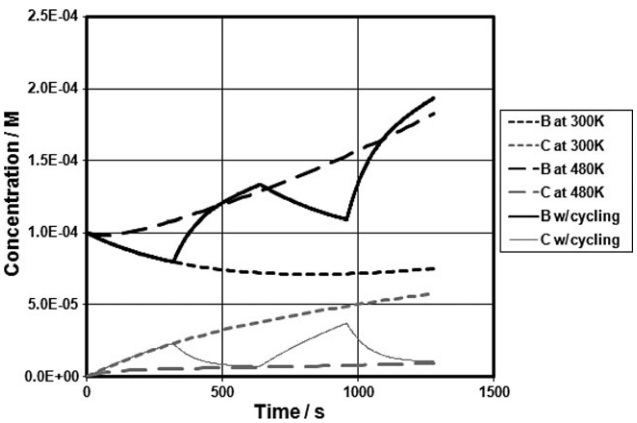

Fig. 7 Concentrations of products **B** and **C** predicted from the **ABC** model (Fig. 4 and Fig. 5) at fixed temperatures and with thermal cycling during the earliest stages of the reactions.

increasing the overall rate of production of **C**. An examination of the changes in concentration of **B** and **C** under steady state and thermal cycling at the earliest times shows an exponential increase in **C** and the autocatalytic activity of **B**. Fig. 7 shows that temperature switching increases the concentration of **B** over steady state temperature levels within the first two thermal cycles; at the first instance of switching from 300 to 480 K, there is a higher concentration of **C** than at 480 K alone, and this higher concentration of **C** drives the formation of **B** to a higher concentration under thermal cycling than at 480 K alone. In addition, with thermal cycling, the concentration of **C** begins to increase over steady state values after six cycles (not shown).

Further verification of the behavior of this system under thermal oscillation was sought by examining the conditions for this model using the Chemical Kinetics Simulator (CKS) program from IBM[13] (not shown). This stochastically-based program predicted the same results as those generated by the Kintecus program.

The **ABCD** model was designed to demonstrate the applicability of thermal cycling in another more general chemical system, in which the target product, **D**, does not participate in feedback and autocatalysis. The model and typical results are shown in Fig. 8 and Fig. 9, respectively. In this model, we explored a shorter reaction time course with a rapid temperature cycle. Product **D** was formed more rapidly under thermal cycling. The **ABCD** model also predicted that, as expected, if the concentration of **A** was not constant, the concentration of **A** would become limiting for the formation of **D** over time (not shown).

Reaction Step	A	E_a	k (at 300K)	k (at 480K)
(1) A + B ⟶ C + D	20.0	50.0	3.94×10^{-8}	7.25×10^{-5}
(2) A + B + Y ⟶ C + D + Y	20.0	1.0	1.34×10^{1}	1.56×10^{1}
(3) C ⟶ 2 B	1.0	18.0	7.34×10^{-4}	1.10×10^{-2}
(4) X ⟶ Y	1.0	2.0	4.48×10^{-1}	6.06×10^{-1}
(5) Y ⟶ X	100.0	10.0	1.82×10^{0}	8.16×10^{0}

Initial concentrations

[A] = 1 M (NB: not constant)
[X] = 1×10^{-3} M
[B] = 1×10^{-4} M

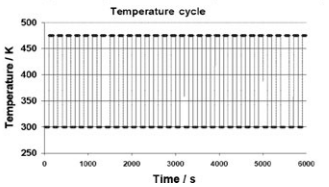

Fig. 8 A description of the **ABCD** model. Inputs include reaction steps and kinetic parameters, A (the Arrhenius constant), E_a, the initial concentrations and the thermal cycling profile. The cycle time is 200 s. with equal time spent at 300 and 475 K; there are 30 cycles over the 6000 s time course.

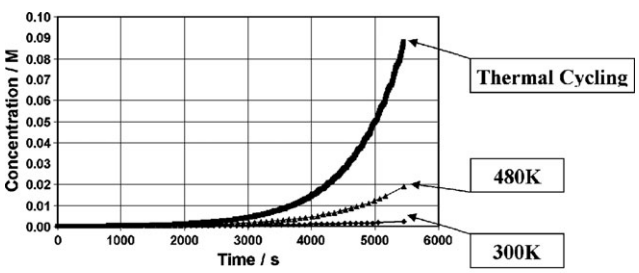

Summary
Concentrations (Molar) of B, C and D after 5460 sec

	Thermal cycling	300K	480K
D	8.77×10^{-2}	2.20×10^{-3}	1.19×10^{-2}
B	4.87×10^{-2}	9.32×10^{-3}	1.61×10^{-2}
C	1.70×10^{-2}	4.34×10^{-4}	1.52×10^{-3}

Fig. 9 Predictions from the **ABCD** model. The results include the concentrations of target product **D** after the model has run under fixed temperature conditions (300 and 480 K) *vs.* under a thermal cycling profile. The concentrations of **B**, **C** and **D** predicted by the model are summarized.

Conclusions

A hallmark of systems chemistry is the fundamental realization that complex behavior of even simple interacting reactions may not be easily reduced to understanding the activities of their individual constituents. Forced, external cycling conditions may cause interactions within chemical systems, resulting in non-linear behavior that may best be explored with computational models. Our computational models display a counter-intuitive behavior under thermal cycling, and further analysis of these systems is likely to assist in creating novel applications that will be particularly exciting in chemical, biochemical and chemical engineering systems.

As of now, the vast majority of chemical reactions are conducted under fixed, constant conditions. Unlike spontaneous oscillating reactions, the models explored here describe systems carried out under fast, forced thermal cycling conditions. Studies of thermal cycling have included investigations of systems where forced oscillating changes in reactant concentrations created non-linear behaviors, and other studies that demonstrated how cycling conditions could drive chemical systems far from equilibrium.[14–16] Recently, a similar chemical model system was described, in which thermal cycling accelerated reaction rates.[17]

Real applications of thermal cycling in chemical systems are rare; however, under the right conditions, exploring cycling conditions may be valuable in synthetic chemistry. For example, thermal cycling may be particularly advantageous in template-directed organic chemistry,[18] and in devising more specific, efficient "one-pot" reaction systems with higher yields and better atom economy.[19] In addition, our models suggest applications for breaking chiral symmetry that may provide insight into new concepts related to prebiotic chemistry.[20,21] For example, in a prebiotic setting, breaking chiral symmetry might arise from long-term, forced oscillating conditions. Diurnal variations of temperature and light, or variations in concentrations because of cycles of wet and dry conditions, might amplify a small initial imbalance in the chirality of molecular populations. Our models support the speculation of C. Viedma who suggested that cycles of dissolution and growth of crystals in a racemic mixture under grinding conditions might break chiral symmetry giving rise to chiral amino acids and sugars.[20,21]

In biosynthesis, thermal cycling has been demonstrated to be important in enzyme-encapsulated hydrogel beads; changes in temperature change the bead volume reversibly, bringing external reactants into the bead and forcing the product out.[22,23] In addition, an important variation on PCR uses a two-temperature thermal cycling protocol to replicate DNA.[24]

We are exploring models of two-temperature PCR that may be valuable in interpreting data in these biochemical systems.

In chemical engineering, microreactors have been designed, in which the oxidation of CO under fast forced oscillating temperatures has a faster reaction rate than under steady state conditions.[25–27] Our computational models may provide a mechanism to explain and optimize this paradoxical behavior, and extend thermal cycling to the design of other novel microreactors.

Our models indicate that simple chemical systems may display paradoxical behavior under thermal cycling. We are investigating the interaction of the different parameters of these models, including the frequency and patterns of thermal cycling, and the kinetic factors that define the steps of such chemical systems. Although these chemical systems are simple, their non-linear behavior under thermal cycling will be challenging to characterize. As we continue to extend our computational models and find optimal parameters for thermal cycling, we are seeking real applications that may be valuable in chemistry and chemical engineering.

Acknowledgements

We gratefully acknowledge funding through the University of New Haven Faculty Research Support to C. B. and P. M. S. We thank our colleagues—Dr George Wheeler and Dr Brad Garber—for thoughtful comments. We thank our students—Ryan Kerick, Melody Johnson, Devon McCarthy, Matt Porto, Thomas Gordon, Caitlin Engle, Christine Stants and Alice Coppock—for their work on this project. We thank the University, the Connecticut Business and Industry Association, and Pfizer, Inc. for supporting student research.

References

1 R. F. Ludlow and S. Otto, *Chem. Soc. Rev.*, 2008, **37**, 101.
2 M. Kindermann, I. Stahl, M. Reimold, W. M. Pankau and G. von Kiedrowski, *Angew. Chem., Int. Ed.*, 2005, **44**, 6750.
3 P. Compain, V. Desvergnes, C. Ollivier, F. Robert, F. Suzenet, M. Barboiu, P. Belmont, Y. Blériot, F. Bolze, S. Bouquillon, E. Bourguet, B. Braida, T. Constantieux, L. Désaubry, D. Dupont, S. Gastaldi, F. Jérome, S. Legoupy, X. Marat, M. Migaud, N. Moitessier, S. Papot, F. Peri, M. Petit, S. Py, E. Schulz, I. Tranoy-Opalinski, B. Vauzeilles, P. Vayron, L. Vergnes, S. Vidal and S. Wilmouth, *New J. Chem.*, 2006, **6**, 823.
4 J. M. R. Parrondo, in *EEC HC&M Network on Complexity and Chaos (#ERBCHRX-CT940546)*, ISI, Torino, Italy, 1996, unpublished.
5 G. P. Harmer and D. Abbott, *Stat. Sci.*, 1999, **14**, 206213.
6 G. P. Harmer and D. Abbott, *Nature*, 1999, **402**, 866.
7 The official Parrondo's paradox website: http://www.eleceng.adelaide.edu.au/Groups/parrondo/.
8 A. P. Flitney and D. Abbott, *Physica A*, 2003, **324**, 152.
9 J. M. R. Parrondo, G. P. Harmer and D. Abbott, *Phys. Rev. Lett.*, 2000, **85**, 5226.
10 J. M. R. Parrondo and L. Dinis, *Contemp. Phys.*, 2004, **45**, 147.
11 H. Martin and H. C. von Baeyer, *Am. J. Phys.*, 2004, **72**, 710.
12 J. C. Ianni, *Kintecus, Windows Version 3.953*, 2008 (available at: http://www.kintecus.com (Kintecus manual available at: http://www.kintecus.com/Kintecus_V395.pdf)).
13 W. Hinsberg and F. Houle, *Chemical Kinetics Simulator (CKS) 1.01*, IBM Almaden Research Centre, San Jose, CA, USA (available at: http://www.almaden.ibm.com/st/computational_science/ck/?cks).
14 W. Vance and J. Ross, *J. Chem. Phys.*, 1995, **103**(7), 2472.
15 M. Tsuchiya and J. Ross, *Proc. Natl. Acad. Sci. U. S. A.*, 2003, **100**(17), 9691.
16 R. D. Astumian, B. Robertson, R. S. Li and J. Ross, *J. Chem. Phys.*, 1992, **96**(9), 6536.
17 C. Antoine and A. Lemarchand, *J. Chem. Phys.*, 2007, **126**(10), 104103.
18 *Templated Organic Synthesis*, ed. F. Diederich and P. J. Stang, Wiley-VCH, Weinheim, 1999.
19 S. J. Broadwater, S. L. Roth, K. E. Price, M. Kobaslija and D. T. McQuade, *Org. Biomol. Chem.*, 2005, **3**, 2899.
20 C. Viedma, *AlbaNova Conference (Origins of Homochirality)*, 2008 (available at: http://agenda.albanova.se/conferenceDisplay.py?confId=322).
21 C. Viedma, *Astrobiology*, 2007, **7**(2), 312.
22 T. G. Park. and A. S. Hoffman, *Biotechnol. Bioeng.*, 1990, **35**(2), 152.
23 T. G. Park and A. S. Hoffman, *Enzyme Microb. Technol.*, 1993, **15**(6), 476.
24 M. F. Kramer and D. M. Coen, *Curr. Prot. Mol. Biol.*, 2001, 15.1.1.
25 H. A. Hansen, J. L. Olsen, S. Jensen, O. Hansen and U. J. Quaade, *Catal. Commun.*, 2006, **7**, 272.
26 J. J. Brandner, G. Emig, M. A. Liauw and K. Schubert, *Chem. Eng. J.*, 2004, **101**, 217.
27 S. Jensen, J. L. Olsen, S. Thorsteinsson, O. Hansen and U. J. Quaade, *Catal. Commun.*, 2007, **8**, 1985.